Journal of Power Sources 196 (2011) 7048–7055

Contents lists available at ScienceDirect

Journal of Power Sources

journal homepage: www.elsevier.com/locate/jpowsour

Study on electrochemically deposited Mg metal

Masaki Matsui*

Materials Research Department, Toyota Research Institute of North America, 1555 Woodridge Ave., Ann Arbor, MI 48105, USA

ARTICLE INFO

Article history:
Received 13 August 2010
Received in revised form
19 November 2010
Accepted 25 November 2010
Available online 2 December 2010

Keywords:
Rechargeable magnesium battery
Electrodeposition
Dendrite
Overpotential

ABSTRACT

An electrodeposition process of magnesium metal from Grignard reagent based electrolyte was studied by comparing with lithium. The electrodeposition of magnesium was performed at various current densities. The obtained magnesium deposits did not show dendritic morphologies while all the lithium deposits showed dendritic products. Two different crystal growth modes in the electrodeposition process of magnesium metal were confirmed by an observation using scanning electron micro scope (SEM) and a crystallographic analysis using X-ray diffraction (XRD). An electrochemical study of the deposition/dissolution process of the magnesium showed a remarkable dependency of the overpotential of magnesium deposition on the electrolyte concentration compared with lithium. This result suggests that the dependency of the overpotential on the electrolyte concentration prevent the locally concentrated current resulting to form very uniform deposits.

1. Introduction

Electrochemical energy storage devices are key components for innovative power train systems such as PHV, FCHV and EV. Especially for a long mile range EV, the energy density of the battery system is very critical. The battery system for the EV requires significantly higher energy density than that of state-of-art Li-ion battery. Therefore, finding new battery chemistry is very important as a future energy source for the EV [1].

For the high energy battery system, rechargeable lithium batteries using lithium metal have been studied for a long time, because of the high specific capacity of lithium metal; 2061 mAh cm^{-3} [2]. One of the major challenges for the lithium metal anode is the prevention of dendrite growth at the surface of the anode which has the possibility to lead a poor cycle performance and safety concerns [3]. Therefore, there has been extensive research on surface treatment, electrolyte additives, and solid state electrolytes to overcome this challenge [4,5].

We believe magnesium metal, which also has high specific capacity; 3833 mAh cm^{-3}, is another example of a potentially high capacity anode active material for the high energy battery system. To our knowledge, only a few research groups have studied to understand the electrochemical behavior of magnesium metal to confirm if it has the same issue of dendrite growth. Gregory et al. [6] have studied various kinds of Grignard reagent based electrolyte solutions and reported that the electro deposited magnesium obtained from organomagnesium chloride/$AlCl_3$ solution in THF showed dendritic morphology in a particular electrolyte composition.

Aurbach et al. have been studying deposition/dissolution mechanism of magnesium by using various analytical techniques; SEM, EQCM, *in situ* FTIR, *in situ* STM, NMR and so on [7–15]. Nakayama et al. [16] have characterized the electrochemical active species in the electrolyte solution by using NMR and Soft X-ray XAS. However among all of these papers, the dendrite formation process of electrodeposited magnesium has never been discussed. Furthermore there has been no systematic study to compare electrochemically deposited magnesium and lithium as anode active materials for a rechargeable battery system.

In the present study, electrodeposition of magnesium and lithium were performed and discussed how the deposition process affects to the morphology of deposits. Also the crystallographic study of the electrodeposited magnesium was conducted to discuss the crystal growth process of the magnesium during electrodeposition.

2. Experimental

In this study, all the electrochemical process of magnesium and lithium were performed by using a three electrode cell in a glove box filled with high purity argon. A polished platinum disc was used as the working electrode for the magnesium deposition and magnesium foil was used as the reference and the counter electrode. An electrolyte solution for magnesium deposition was prepared by mixing 1 ml of 2 M ethylmagnesium chloride in tetrahydrofuran (Sigma–Aldrich), 0.37 ml of dimethylaluminum chloride

* Tel.: +1 734 995 5313; fax: +1 734 995 2459.
E-mail address: masaki.matsui@tema.toyota.com

0378-7753/$ – see front matter © 2010 Elsevier B.V. All rights reserved.
doi:10.1016/j.jpowsour.2010.11.141

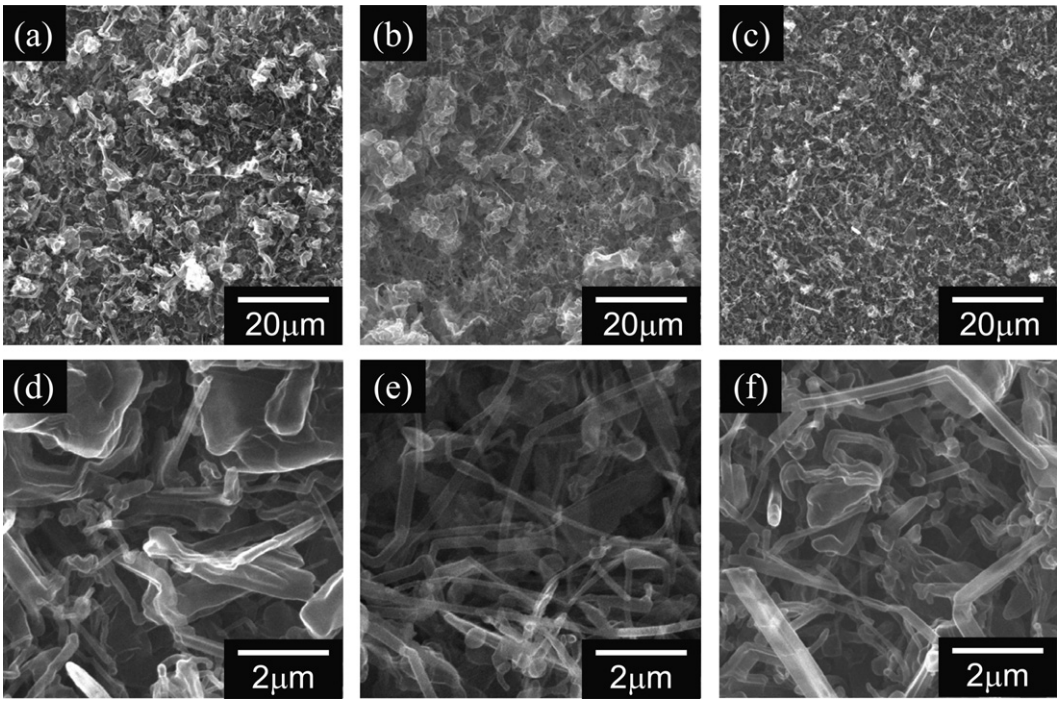

Fig. 1. SEM images of the electrodeposited lithium (a) 500×, 0.5 mA cm^{-2}, (b) 500×, 1.0 mA cm^{-2}, (c) 500×, 2.0 mA cm^{-2}, (d) 5000×, 0.5 mA cm^{-2}, (e) 5000×, 1.0 mA cm^{-2} and (f) 5000×, 2.0 mA cm^{-2}.

(Sigma–Aldrich) and anhydrous tetrahydrofuran (Sigma–Aldrich) [17]. The mixed solution was stirred for 24 h before the electrochemical measurements.

The electrodeposition of lithium was performed by using well polished nickel disc as a working electrode. Lithium foil was used as the reference and the counter electrode respectively. A conventional electrolyte solution; ethylene carbonate (EC) and diethyl carbonate (DEC) mixed solvent containing 1 M of lithium hexafluorophosphate ($LiPF_6$) purchased from Mitsubishi Chemical was used for the electrodeposition of lithium.

The electrodeposition of the magnesium and lithium was carried out by galvanostatic method under three different current densities; 0.5, 1.0 and 2.0 mA cm^{-2}. The electrodeposition processes were terminated by total electric charge at 1 C cm^{-2}. After the electrodeposition, the magnesium deposits were immediately rinsed with THF for 3 times to remove electrolyte solution and transferred to SEM by using special sample holder to avoid an exposure of the sample into air. In the case of the lithium, obtained specimens were rinsed with DEC instead of THF and transferred to SEM by following the same procedure as magnesium specimens.

The XRD analysis of the magnesium deposits were carried out with Cu-Kα beam (40 kV, 100 mA) at a scan rate 2° min^{-1} in the 2θ range 20–70°. In order to study the crystal orientation of the magnesium deposits, pole-figure measurement for (0 0 2) diffraction peak which appears 2θ at 34.447° was also performed for each deposit.

3. Result and discussion

SEM images of the lithium deposits are shown in Fig. 1. The lithium deposits obtained at 0.5 mA cm^{-2} and 1.0 mA cm^{-2} showed uneven surface morphology as shown in Fig. 1(a) and (b). Some whisker like lithium deposits (usually called just dendrite) were gathering to form porous deposition products as shown in magnified images (Fig. 1(d) and (e)). The lithium deposits obtained at 2.0 mA cm^{-2} are shown in Fig. 1(c). Although it shows relatively even surface morphology, it can be observed that the lithium deposit also consists of whisker like products as shown in the magnified image (Fig. 1(f)).

On the other hand, the magnesium deposits showed very different surface morphology compared with the lithium deposits as shown in Fig. 2. At first it can be said that all the magnesium deposits did not show a typical dendritic morphology in these three deposition conditions while all the lithium deposits showed dendritic and porous deposits. Fig. 2(a) and (b) shows the SEM images of the magnesium deposits obtained at 0.5 mA cm^{-2} and 1.0 mA cm^{-2} respectively. In both images, the magnesium deposits have round shaped grains with uniform size approximately 2–3 μm. The magnified images of these deposits showed that each grain has clear edge which is reflecting the hexagonal structure of magnesium. It indicates that the magnesium deposits have high crystallinity. The SEM images of the magnesium deposit obtained at 2.0 mA cm^{-2} are shown in Fig. 2(c). The magnesium deposit obtained at 2.0 mA cm^{-2} showed very different surface morphology from other two specimens. The specimen showed relatively small grains which are approximately had 0.5–1 μm resulting to form more smooth surface morphology and dense deposit comparing with other two deposits. The shape of each grain can be observed in the magnified images as shown in Fig. 2(f). The grains also had edges reflecting the crystal structure of magnesium however the observed grains had mainly triangle shape which suggests that the magnesium deposit obtained at 2.0 mA cm^{-2} could have different crystal orientation from other two specimens.

A crystallographic study for the magnesium deposits were performed by using XRD. Fig. 3 shows XRD patterns of the magnesium deposits. All the diffraction patterns showed peaks which is corresponding to magnesium or platinum which was used as substrate. According to the powder diffraction file PDF#04-003-2526, (0 0 2) diffraction which appears at 34.447° has 26.9% of the intensity of (1 0 1) diffraction at 36.630°. In the case of the magnesium deposits obtained at 0.5 mA cm^{-2} and 1.0 mA cm^{-2}, however, the intensity of (0 0 2) diffraction showed 81% and 77% of peak intensity compared with (1 0 1) diffraction respectively as shown in Fig. 3(a) and (b). Hence, it can be said that these magnesium deposits have (0 0 1)

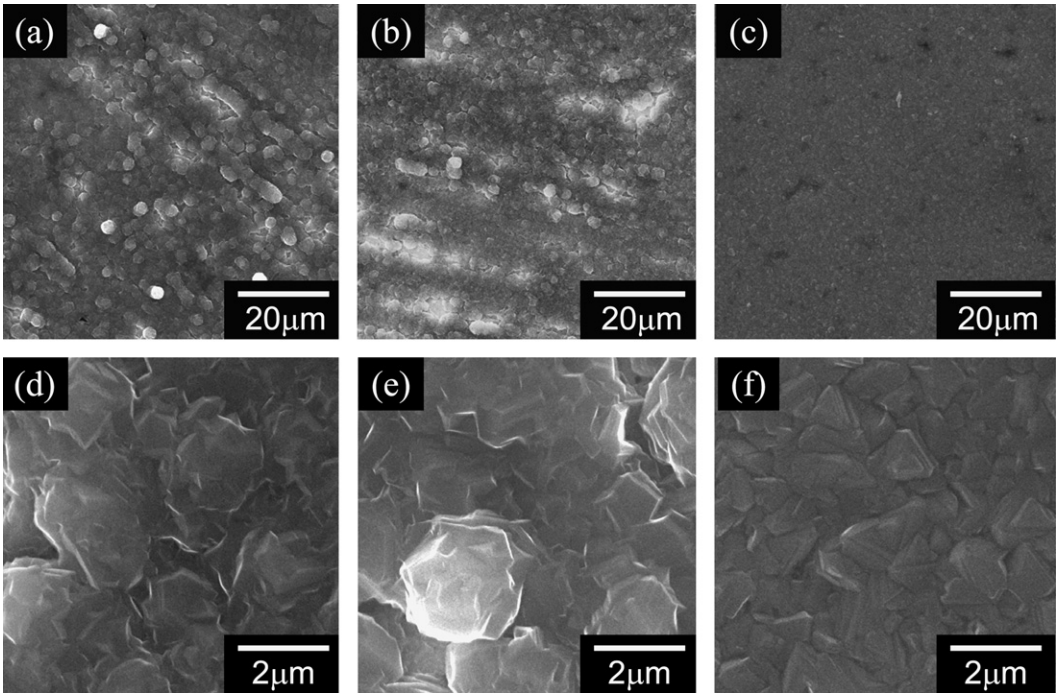

Fig. 2. SEM images of the electrodeposited magnesium (a) 500×, 0.5 mA cm^{-2}, (b) 500×, 1.0 mA cm^{-2}, (c) 500×, 2.0 mA cm^{-2}, (d) 5000×, 0.5 mA cm^{-2}, (e) 5000×, 1.0 mA cm^{-2} and (f) 5000×, 2.0 mA cm^{-2}.

preferred orientation. On the contrary, (0 0 2) diffraction of the magnesium deposit obtained at 2.0 mA cm^{-2} showed 27% of (1 0 1) diffraction intensity which is almost same as powder diffraction file (Fig. 3(c)). Furthermore, (1 0 0) diffraction and (1 1 0) diffraction showed 61.8% and 18.6% of (1 0 1) diffraction intensity while the powder diffraction file shows 24.7% and 13.8% respectively. This result supports the hypothesis discussed in SEM observation, that the magnesium deposit obtained at 2.0 mA cm^{-2} has different crystal orientation compared with other two specimens.

Pole figure measurements of (0 0 2) diffraction for these specimens were carried out to confirm the crystal orientation of these specimens. Fig. 4 shows (0 0 2) pole figures of the electrodeposited magnesium specimens normalized by the highest peak intensity of each measurement. Although the highest peak intensity of each specimen was observed at 30–40° from the center (ND), relatively high intensity was also observed at ND of the magnesium deposited at 0.5 mA cm^{-2} and 1.0 mA cm^{-2}. It shows that these two specimens partially have (0 0 1) preferred orientation. On the other hand, since the magnesium specimen obtained at 2.0 mA cm^{-2} did not show high intensity at ND, it could be said that the magnesium does not have (0 0 1) preferred orientation. Considering the intensity of diffraction discussed above, it indicates that the magnesium deposited at 2.0 mA cm^{-2} has (1 0 0) preferred orientation.

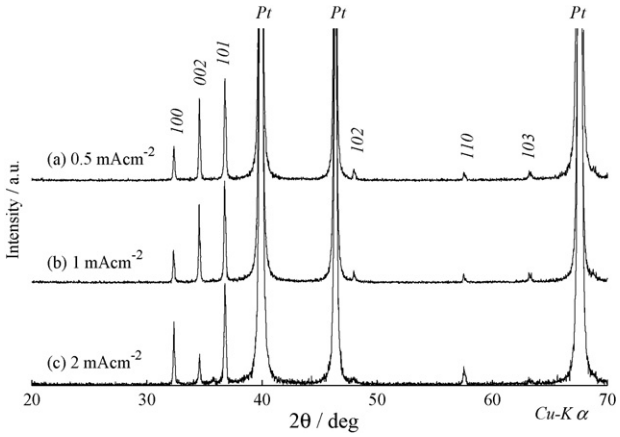

Fig. 3. XRD patterns of the electrodeposited magnesium, (a) 0.5 mA cm^{-2}, (b) 1.0 mA cm^{-2} and (c) 2.0 mA cm^{-2}.

Based on the results obtained by SEM observation and XRD study, we think that the electrodeposition process of magnesium can be categorized into two crystal growth modes which are dependent on current density as follows. At low current density (0.5 mA cm^{-2} and 1.0 mA cm^{-2}), the deposition rate is determined by the charge transfer reaction. Also the crystal growth speed of the magnesium deposit is enough slow. Therefore the deposited magnesium atoms have enough time to diffuse at the surface of the electrode so that each grain of the magnesium deposit grows by minimizing the surface energy. In the case of magnesium, the *ab*-plane in its hcp structure can be considered as a crystal plane which has the lowest surface energy, according to Wolff's broken bond model [18]. As a consequence the magnesium deposit obtained at low current density shows (0 0 1) preferred orientation. At high current density (2.0 mA cm^{-2}), however, the mass transfer of electrochemically active magnesium determines the deposition rate rather than charge transfer, hence the deposited magnesium atoms do not have enough time to diffuse at the surface of the electrode and must be incorporated into the crystal structure immediately. Therefore the crystal growth rate of the magnesium deposit needs to be maximized. Consequently the *ab*-plane of the magnesium grows perpendicular (or with certain angle) to the substrate, because the crystal growth rate within *ab*-plane is generally faster than that of other planes in the case of hexagonal structure.

The above discussion can be summarized shortly as follows. It was confirmed that the electrodeposited magnesium does not show dendritic morphology in three deposition conditions which we carried out, while lithium deposits formed dendritic morphology in the same electrochemical conditions. The morphology of the magnesium deposit could be affected by the process which limits the

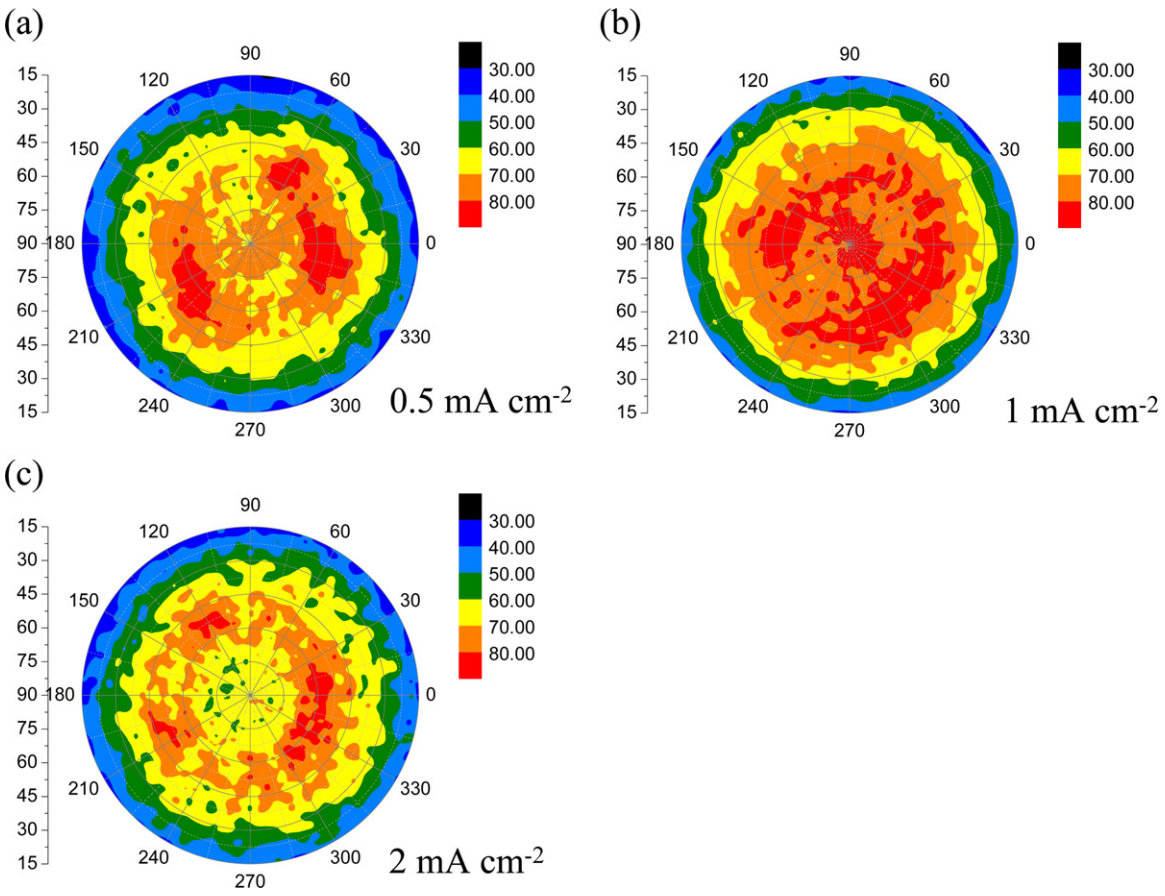

Fig. 4. (0 0 2) pole figure of the electrodeposited magnesium, (a) 0.5 mA cm^{-2}, (b) 1.0 mA cm^{-2} and (c) 2.0 mA cm^{-2}.

deposition rate. This result was encouraging to apply magnesium metal as an anode active material for rechargeable magnesium battery.

However further discussions are required to answer the question why magnesium does not form dendrite. At first, the difference in the surface chemistry between lithium and magnesium deposits needs to be discussed. In the case of lithium deposition, it is well know that the electrolyte solution is reduced resulting to form solid electrolyte interphase (SEI) layer [19]. Since an inhomogeneous SEI layer can be easily formed, the current density of lithium deposition can be easily focused at a particular site which has relatively low resistance in the SEI layer resulting to initiate the dendrite growth. On the other hand, it was reported that SEI was not formed during the electro deposition of magnesium metal [12]. Fig. 5 shows the chronopotentiograms of lithium and magnesium deposition during the first 1 min of the deposition process. In the case of lithium deposition, the electrode potential for lithium deposition gradually declined by showing positive value against the lithium metal for 15 s. Once the electrode potential reached at −0.18 V vs. Li, the electrode potential stopped declining after 19 s as shown in Fig. 5(a). On the other hand, the electrode potential for the magnesium deposition immediately reached to −0.95 V vs. Mg and started rising (Fig. 5(b)). It suggests that the SEI formation takes place in the beginning of the lithium deposition process, while the deposition of magnesium immediately occurs without the formation of SEI layer.

In addition we think the coulombic efficiency of the deposition processes also affects to the morphology of the deposits. Fig. 6 shows the electric charge during the cyclic voltammetry for lithium and magnesium. In the case of lithium, the coulombic efficiency of lithium deposition/dissolution process showed 86.1% at the 1st cycle and 91.9% in following cycles as shown in Fig. 6(a). It suggests a continuous reduction of the electrolyte solution takes place during the lithium deposition/dissolution process. Meanwhile the deposition/dissolution process of magnesium showed 99.3% coulombic efficiency at the 1st cycle and 99.4% for following cycles. Therefore, there are very few possibilities for the deposition process of magnesium to be interfered by any deposit formed by side reaction. As a result, magnesium deposit can grow very smoothly.

Secondary the electrochemical active species in the electrolyte solution need to be discussed. Aurbach et al. reported that an organometallic complex electrolyte based on Grignard reagent has dynamic multiple equilibria among various magnesium species and aluminum species [20]. Therefore it is natural to expect that the EtMgCl–2Me_2AlCl complex electrolyte which was used for this study also contains various species formed by multiple equilibria such as Schlenk equilibrium (i.e. 2EtMgCl $\rightleftarrows$ $Et_2Mg + MgCl_2$), transmetalation reactions (e.g. $EtMgCl + Me_2AlCl \rightleftarrows MgCl^+ + EtMe_2AlCl$) and the formation of dimer specie (i.e. $Mg_2Cl_3^+ \rightleftarrows MgCl^+ + MgCl_2$). Author's group also reported that the $Mg_2Cl_3THF_6^+$ is one of the key species for the electrodeposition/dissolution of magnesium [21,22]. In addition, Nakayama et al. [16] have reported that THF also affects to these multiple equilibria. Based on those reports, the kinetics of the electrodeposition/dissolution of magnesium could be determined by the activity of magnesium species in these equilibria.

Accordingly further voltammetric studies for the electrodeposition of lithium and magnesium were carried out particularly focusing on the affect of the electrolyte concentration which determines the activity of the electrochemical active species of lithium or magnesium ion in the electrolyte solution.

The cyclic voltammograms of lithium deposition/dissolution process for 1.0 M $LiPF_6$, 0.10 M $LiPF_6$ and 0.01 M $LiPF_6$ electrolyte

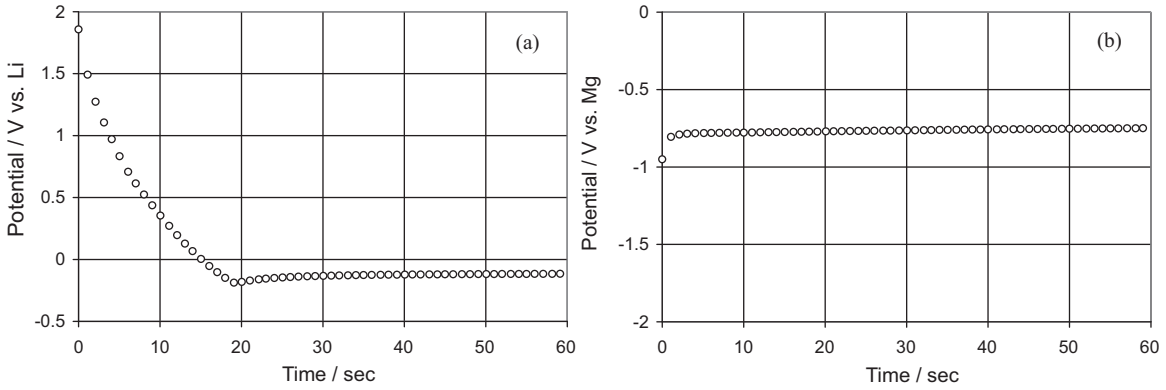

Fig. 5. Chronopotentiograms during the galvanostatic deposition of lithium (a) and magnesium (b) at 0.5 mA cm^{-2}.

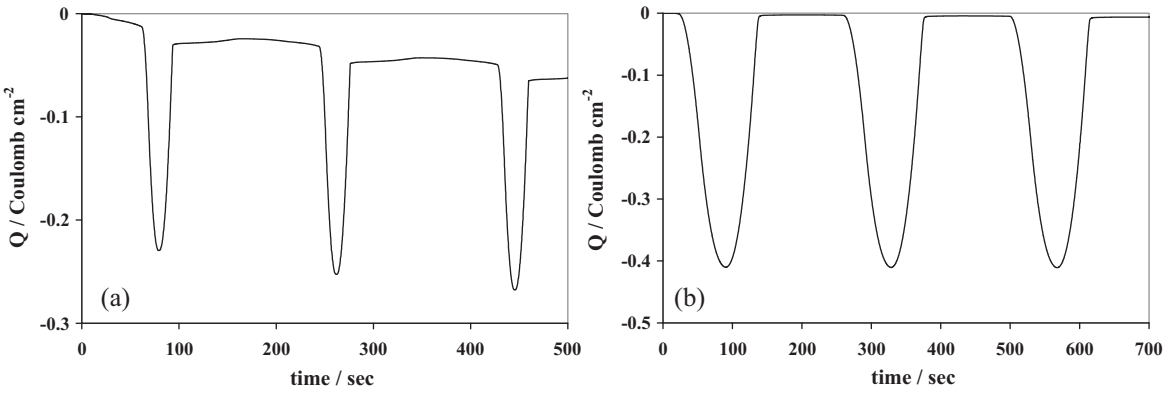

Fig. 6. The electric charge during cyclic voltammetries of lithium and magnesium deposition/dissolution process. (a) Lithium: 3 cycles, 25 mV s^{-1}, −0.5 to 2.0 V vs. Li, 1.0 M $LiPF_6$ in EC:DEC (3:7). (b) Magnesium: 3 cycles, 25 mV s^{-1}, −1.0 to 2.0 V vs. Mg, 0.25 M EtMgCl–2Me_2AlCl in THF.

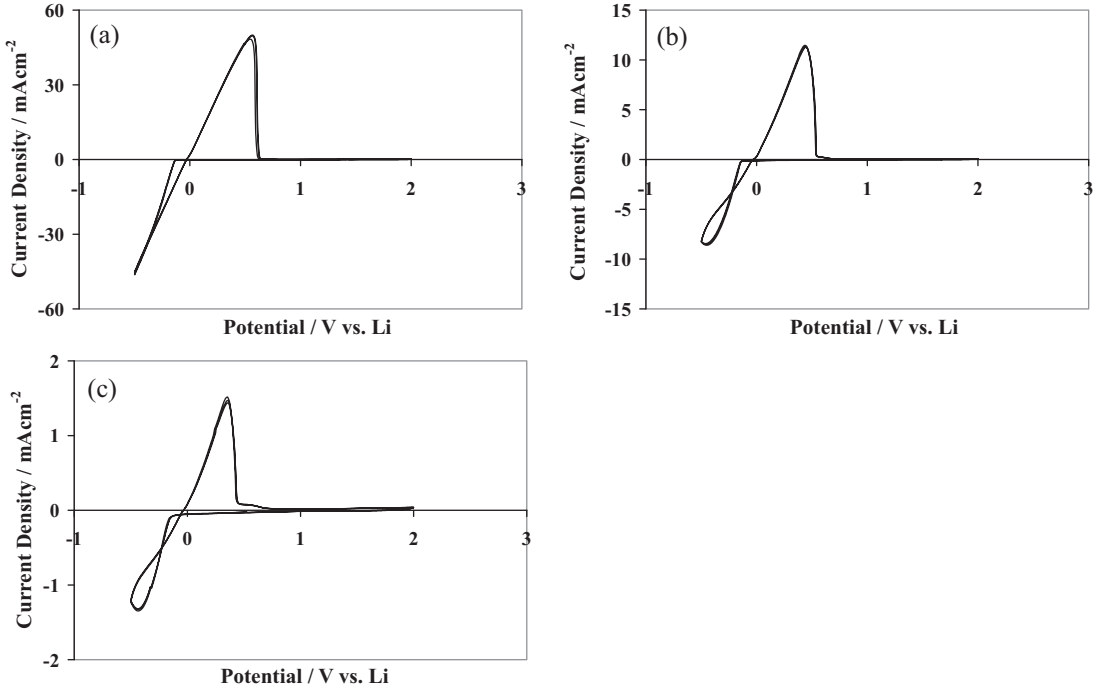

Fig. 7. Cyclic voltammograms of the lithium deposition/dissolution process: 3 cycles, 25 mV s^{-1}, −0.5 to 2.0 V vs. Li (a) 1.0 M $LiPF_6$ in EC:DEC (3:7), (b) 0.10 M $LiPF_6$ in EC:DEC (3:7), (c) 0.01 M $LiPF_6$ in EC:DEC (3:7).

Table 1
Overpotential for the initial deposition of the lithium on nickel substrate and overpotential of the lithium deposition at 1 mA cm^{-2} for deposition current.

	Concentration		
	1.0 M	0.10 M	0.01 M
Initial deposition	0.139 V	0.137 V	0.157 V
1 mA cm^{-1}	0.145 V	0.161 V	0.299 V

Table 2
Overpotential for the initial deposition of the magnesium on platinum substrate and overpotential of the magnesium deposition at 1 mA cm^{-2} for deposition current.

	Concentration		
	0.25 M	0.10 M	0.05 M
Initial deposition	0.248 V	0.698 V	0.845 V
1 mA cm^{-1}	0.294 V	1.118 V	2.706 V

solutions are shown in Fig. 7. Although the current density of the deposition/dissolution process decreased with the decrease of the electrolyte concentration, the overpotential of the initial lithium deposition on nickel did not change so much. The overpotential of the initial lithium deposition on nickel with 0.01 M $LiPF_6$ solution shown in Fig. 7(c) was 0.157 V while the overpotential of 1.0 M solution was 0.139 V (Fig. 7(a)). Even with 100 times lower electrolyte concentration, the difference of the overpotential between these two conditions was only 26 mV between these two solutions. The over potential at the deposition current 1 mA cm^{-2} during cathodic sweep for each electrolyte was also compared for these electrolyte solutions as shown in Table 1 together with the overpotential of initial lithium deposition on nickel electrode. In the case of 0.10 M solution, the overpotential at 1 mA cm^{-2} increased up to 0.161 V due to the decreased current density, and 0.01 M solution showed 0.299 V of overpotential at the same current density.

The magnesium deposition/dissolution process showed significantly different electrochemical behavior from lithium. Fig. 8 shows the cyclic voltammograms of magnesium deposition/dissolution process measured with 0.25 M, 0.10 M and 0.05 M of EtMgCl–2Me_2AlCl complex electrolyte solution in THF. The overpotential of the initial magnesium deposition on platinum electrode showed remarkably high dependency on electrolyte concentration. The overpotential of 0.10 M of EtMgCl–2Me_2AlCl solution was 0.698 V while 0.25 M solution showed 0.248 V (Fig. 8(a) and (b)). Moreover the overpotential of 0.05 M solution was 0.845 V as shown in Fig. 8(c). The overpotential at 1.0 mA cm^{-2} during electrodeposition of magnesium also showed strong dependency on the electrolyte concentration. Whereas the 0.25 M solution showed 0.294 V of overpotential at 1.0 mA cm^{-2} deposition current, the 0.10 M solution showed 1.118 V of overpotential. Since the deposition current never reached to 1 mA cm^{-2} within the range of CV measurement in the case of 0.05 M solution, the overpotential at 1.0 mA cm^{-2} deposition current was estimated as 2.706 V by extending the slope of the deposition. The overpotential values for initial deposition and 1.0 mA cm^{-2} for each electrolyte solution were summarized in Table 2. This result shows that the deposition/dissolution process of magnesium has much higher dependency on the activity of the electrochemical active species in comparison with the lithium.

We assume this phenomenon is strongly related to the equilibrium of various species in the solution. Once the activity of one species changes, the activity of all the other species need to be changed to come back to the equilibrium. Therefore this process always involves some reaction such as transmetalation. As a result the kinetics of the electrodeposition of magnesium could be determined by the kinetics of equilibrium we discussed in above.

Based on the above discussion, a possible mechanism which may explain the reason why the magnesium did not form dendritic deposition product. During the electrodeposition process of magnesium, at first the electron transfer from electrode to electrochemically active species occurs at a local site of the electrode surface resulting to form the first deposit such as a nucleation. At the moment the deposition occurs, the activity of the electrochemical

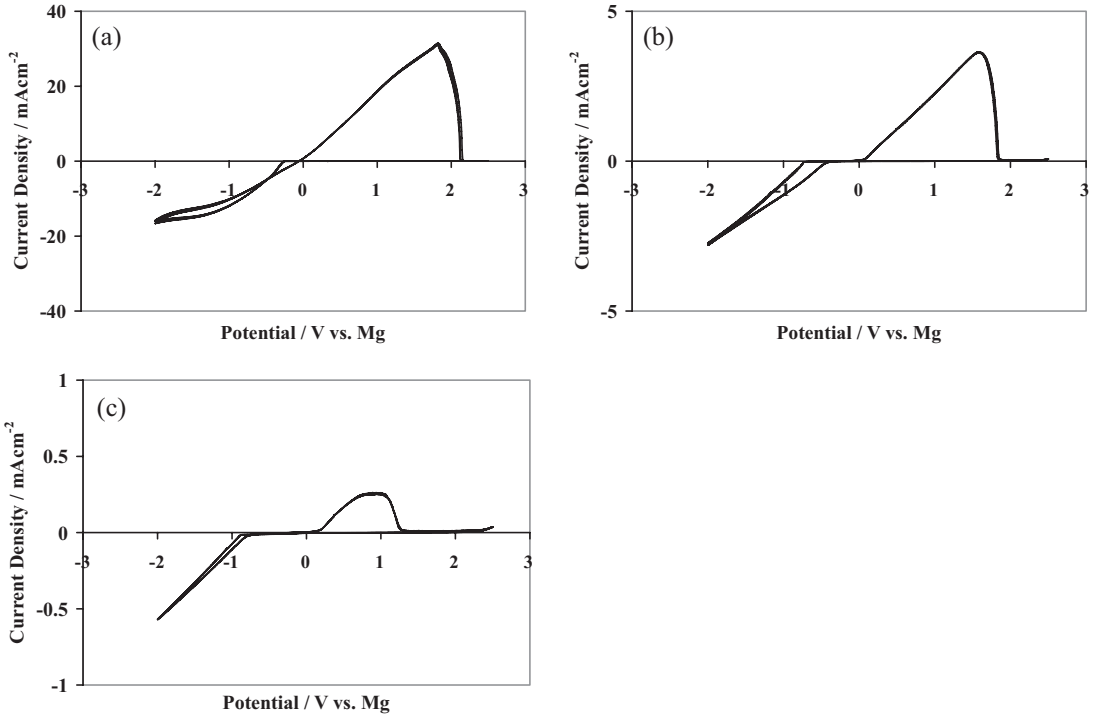

Fig. 8. Cyclic voltammograms of the magnesium deposition/dissolution process: 3 cycles, 25 mV s^{-1}, −2.0 to 2.5 V vs. Mg (a) 0.25 M EtMgCl–2Me_2AlCl in THF, (b) 0.10 M EtMgCl–2Me_2AlCl in THF, (c) 0.05 M EtMgCl–2Me_2AlCl in THF.

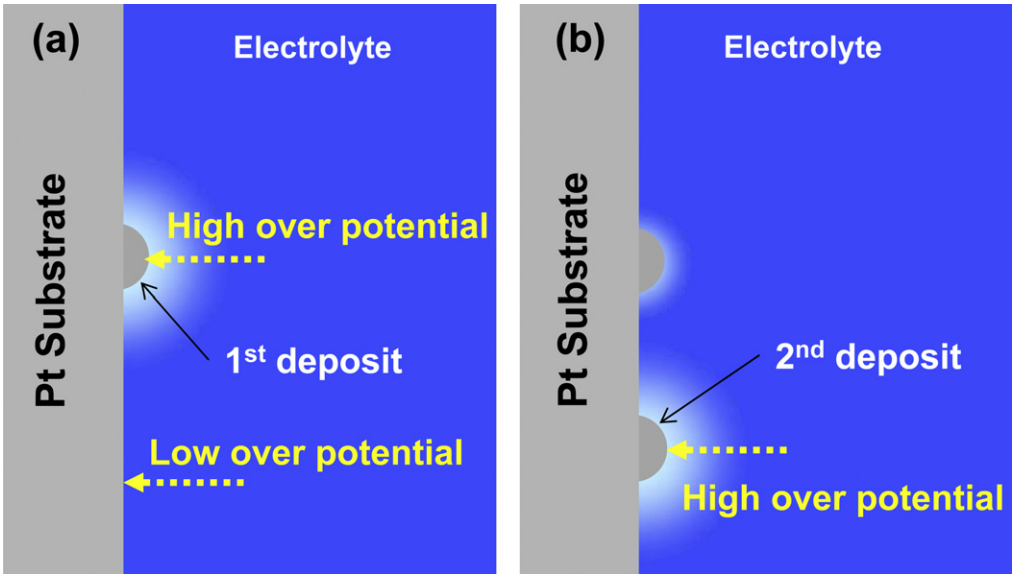

Fig. 9. Schematic image of magnesium deposition process (a) after the first deposition, (b) after the following deposition (color of the electrolyte represents the concentration).

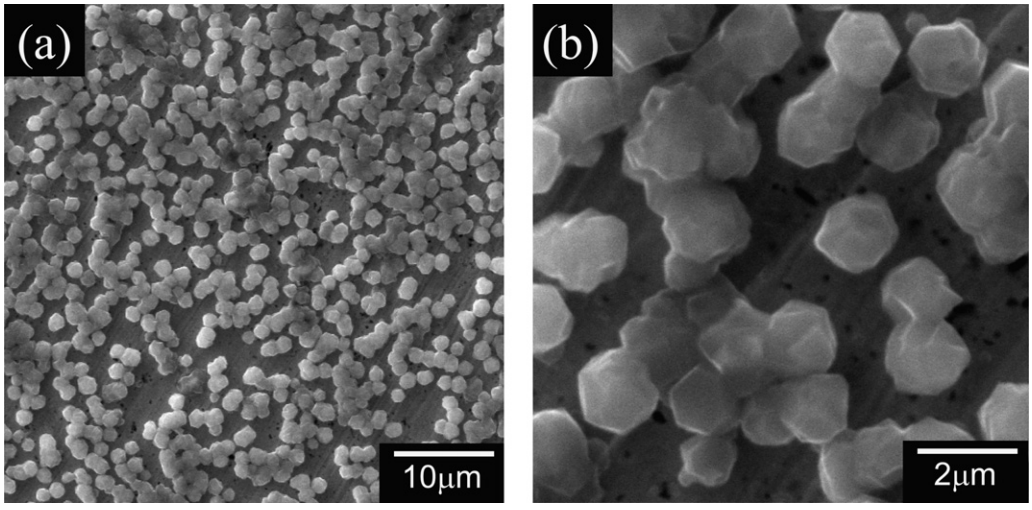

Fig. 10. SEM images of the electrodeposited magnesium deposited at 0.5 mA cm^{-2} for 500 s (0.25 C cm^{-2}), (a) 1000× and (b) 5000×.

active species surrounding the magnesium deposit decreases even for a very short moment. Since the overpotential of magnesium deposition has high dependency on the activity of the electrochemical active species, the overpotential for further deposition of magnesium on the first deposits significantly increases. Hence another local site at electrode surface becomes a preferred site for the next deposition. A schematic image of the moment after the first deposition is shown in Fig. 9(a). Then the second deposition occurs at another site as shown in Fig. 9(b). By repeating this process, the nucleation of magnesium takes place very randomly and the deposition current cannot be focused on a local area of electrode surface. As a consequence the magnesium deposit forms very uniform deposition product as we observed in the first part of the discussion. Fig. 10 shows SEM images for electrochemically deposited magnesium in the early stage of deposition (0.5 mAh cm^{-2}, 0.25 C cm^{-2}). The magnesium particles with uniform size approximately 1.5 μm were observed in the wide area of the electrode surface. The morphology of the magnesium deposits suggests that the random nucleation process took place at the electrode surface as same as the above hypothesis. Further investigation such as characterization of electrochemical active species and a mechanistic study of magnesium ion transportation in the electrolyte solution will be necessary to prove it.

4. Conclusion

The electrodeposition process of magnesium from Grignard reagent based electrolyte solution was studied by comparing with lithium. Two different crystal growth modes in the electrodeposition process of magnesium were confirmed by SEM observation and XRD analysis. The magnesium deposit obtained at low current density showed (0 0 1) preferred orientation formed by minimizing surface energy during slow deposition process. On the contrary, the magnesium deposit obtained at high current density showed (1 0 0) preferred orientation formed by maximizing the crystal growth speed for high deposition rate. The obtained magnesium deposits did not show any dendritic morphology while the lithium showed dendritic deposits obtained at the same electrochemical condition.

An electrochemical study of the deposition/dissolution process of the magnesium showed that the overpotential of magnesium deposition has a significantly high dependency on the activity of electrochemical active species. A hypothesis was proposed that the overpotential of magnesium deposition process suppresses a locally focused current which initiates the growth of the deposits with dendritic morphology.

Acknowledgements

The author is grateful for helpful discussions with Dr. Toshihiko Tani and Dr. John Muldoon of Toyota Research Institute of North America.

References

[1] M. Armand, J.-M. Tarascon, Nature 451 (2008) 652–657.
[2] D. Fauteaux, R. Koksbang, J. Appl. Electrochem. 23 (1993) 1–10.
[3] I. Yoshimatsu, T. Hirai, J. Yamaki, J. Electrochem. Soc. 135 (1988) 2422–2427.
[4] K. Kanamura, S. Shiraishi, Z. Takehara, J. Electrochem. Soc. 143 (1996) 2187–2197.
[5] S. Visco, E. Nimon, B. Katz, U.S. Patent No. 7,282,296, October 16th, 2007.
[6] T. Gregory, R.J. Hoffman, R.C. Winterton, J. Electrochem. Soc. 137 (1990) 775–780.
[7] Z. Lu, A. Schechter, M. Moshkovich, D. Aurbach, J. Electroanal. Chem. 466 (1999) 203–217.
[8] D. Aurbach, M. Moshkovich, A. Schechter, R. Turgeman, Electrochem. Solid-State Lett. 3 (2000) 31–34.
[9] D. Aurbach, R. Turgeman, O. Chusid, Y. Gofer, Electrochem. Commun. 3 (2001) 252–261.
[10] D. Aurbach, Y. Cohen, M. Moshkovich, Electrochem. Solid-State Lett. 4 (2001) A113–A116.
[11] D. Aurbach, A. Schechter, M. Moshkovich, Y. Cohen, J. Electrochem. Soc. 148 (2001) A1004–A1014.
[12] D. Aurbach, I. Weissman, Y. Gofer, E. Levi, Chem. Record 3 (2003) 61–73.
[13] Y. Gofer, O. Chusid, H. Gizbar, Y. Viestfrid, H.E. Gottlieb, V. Marks, D. Aurbach, Electrochem. Solid-State Lett. 9 (2006) A257–A260.
[14] Y. Viestfried, O. Chusid, Y. Goffer, P. Aped, D. Aurbach, Organometallics 26 (2007) 3130–3137.
[15] O. Mizrahi, N. Amir, E. Pollak, O. Chusid, V. Marks, H. Gottlieb, L. Larush, E. Zingrad, D. Aurbach, J. Electrochem. Soc. 155 (2008) A103–A109.
[16] Y. Nakayama, Y. Kudo, H. Oki, K. Yamamoto, Y. Kitajima, K. Noda, J. Electrochem. Soc. 155 (2008) A754–A759.
[17] H. Oki, Y. Nakayama, K. Noda, Japanese Patent, P2007-188709A.
[18] G.A. Wolff, J.D. Boder, CNRS (1965) 172–194.
[19] E. Peled, J. Electrochem. Soc. 126 (1979) 2047–2051.
[20] V. Yulia, C. Orit, G. Yossi, D.A. Pinchas, Organometallics 26 (2007) 3130–3137.
[21] H.S. Kim, J. Muldoon, M. Matsui, 217th ECS Meeting, Vancouver, BC #225.
[22] H.S. Kim, J. Muldoon, 218th ECS Meeting, Las Vegas, NV #315.